A COMPARATIVE STUDY OF GRAPHENATED-CARBON NANOTUBES COTTON AND CARBON NANOTUBES AS CATALYSTS FOR COUNTER ELECTRODE IN DYE-SENSITIZED SOLAR CELLS

Yusnita Yusuf[1], Suhaidi Shafie[1,2*], Ismayadi Ismail[1], Fauzan Ahmad[3], Mohd Nizar Hamidon[1,2], Shyam S. Pandey[4], Nazalea Yazmin Muhammad[1] and Wei Lei[5]

[1]Institute of Nanoscience and Nanotechnology, Universiti Putra Malaysia, 43400 Serdang, Selangor, Malaysia.
[2]Department of Electrical and Electronic Engineering, Faculty of Engineering, Universiti Putra Malaysia, 43400 Serdang, Selangor, Malaysia.
[3]Malaysian-Japan International Institute of Technology, Universiti Teknologi Malaysia, 57000 Kuala Lumpur, Malaysia.
[4]Graduate School of Life Science and System Engineering, Kyushu Institute of Technology, 2-4 Hibikino, Wakamatsu, Kitakyushu, Fukuoka 808-0196, Japan.
[5]School of Electronic Science and Engineering, Southeast University, Sipailou, JinLing Yuan 109, Nanjing 210096, China.

*suhaidi@upm.edu.my

Abstract. This work reports a comparative study of synthesized graphenated-carbon nanotubes cotton (g-CNTC), standard carbon nanotubes (CNTP), and conventional platinum (Pt) thin layer which are employed as the counter electrodes in dye-sensitized solar cells (DSSC). The g-CNTC was synthesized via the floating-catalyst chemical vapor deposition (FCCVD) method. Subsequently, the g-CNTC was made into a uniform paste and deposited for the counter electrode layer. The results obtained from FESEM/TEM, Raman spectroscopy, CV and I-V measurements respectively exposed the structural, graphitization and I-V characteristics. Briefly, the morphology of g-CNTC showed the growth of graphene foliates out-sidewalls of CNT with a diameter of 40 nm. The graphitization of g-CNTC showed two dominant peaks namely the D (1355 cm^{-1}) and G (1608 cm^{-1}) bands with strong intensities. The g-CNTC counter electrode provided good electrical conductivity (3.66×10^{-3} to 6.45×10^{-3} S/cm), which is a significant feature to employ counter electrodes to enhance DSSC performance. In addition, the g-CNTC counter electrode offered an excellent catalytic activity for iodide/triiodide reaction and exhibited 3.49 % of photovoltaic conversion energy, which was much higher compared to CNTP (2.93 %) and platinum (3.12 %), respectively.

Keywords: dye-sensitized solar cells, counter electrodes, carbon-based, graphenated-carbon nanotubes cotton

Article Info

Received 5th October 2021
Accepted 7th December 2021
Published 20th December 2021

ISSN: 1823-7010, eISSN: 2600-7444

Introduction

The third generation of emerging films technology recognizes dye-sensitized solar cells (DSSC) which are the new generations in the fields of photovoltaics. The DSSC were developed by Brian O'Regan and Micheal Grätzel in 1991 [1]. Their significant interest such as easy fabrication, low-cost production, light, affordable source of renewable energy, outstanding performance under the low light condition, and have several options for improving the efficiency [2–7]. The DSSC structure consists of semiconductor photoanode, a sensitizer dye, electrolyte and counter electrode (CE). The CE with catalyst is used for iodide/triiodide reaction, serves to bring the electrons from the external loads connected to the cell and catalyzed the triiodide/iodide reaction in the electrolyte.

The typical CE platinum (Pt) is the most selective CE due to its excellent catalytic activity, and conductivity [8]. The best power conversion of the DSSC was obtained at 12.3% using Cobalt(II/III)-based electrolytes and Pt-based counter electrodes [9]. Despite that Pt-based are still the effective catalyst for a redox reaction, however, their expensive cost makes them less cost-effective. To be regarded as a promising catalyst for CE, a material must meet the following criteria such as excellent electronic conductivity, electrocatalytic activity and/or high active surface area, and high transparency with outstanding compatibility with the transparent conductive oxide (TCO) support. Recent studies have compiled the potential materials to substitute platinum for instance, introducing carbon materials as potential CE including carbon nanotubes (CNT), carbon fibers, carbon black, graphene, and graphite have been provided successful outcomes [10], [11]. Nonetheless, many electrode materials with high catalytic performance do not provide enough electron transfer capability, hence developing hybrid carbonaceous materials will enhance the efficient charge transfer for conducting electrons.

Recently, our group has successfully reported a method producing novel three-dimensional (3D) graphenated-carbon nanotubes cotton (g-CNTC) hybrid [12]. The g-CNTC was synthesized without using any substrate via single-step process of floating-catalyst chemical vapor deposition (FCCVD). The report demonstrated a direct growth of g-CNTC and its effect of hydrocarbon injection rate on the g-CNTC formation for gas sensors application. The result showed that the synthesized g-CNTC hybrid can be potentially applied as an electrode in the electronic device. Inspired by this previous work, we suggest to use g-CNTC hybrid structures as CE and examine its performance for DSSC application. Several studies on g-CNT hybrid have been published such as bilayer graphene/MWCNT [13] and graphene nanosheet/MWCNT [14]. In the report [13], bilayer graphene/MWCNT electrode prepared using double self-assembly method in which graphene flakes layered on top of deposited MWCNT on transparent conductive glass. Meanwhile [14], reported that the electrode was assembled in sandwiched structure with zinc oxide photoanode-based DSSC, and they obtained 4.10% of efficiency. Another study of g-CNT was using high shear exfoliation. The prepared graphene nanosheets were infused into MWCNT by probe sonication and deposited on the substrate. They study on the effect of 3-Aminoproply treithoxysilane on the efficiency performance and obtained 3.08% of efficiency. However, there is insufficient research on g-CNTC formation structure on carbon-based CE.

To the best of our knowledge, there is relatively less attention to the utilization of hybrid g-CNTC synthesized via FCCVD method as CE films for DSSC application. We hypothesized the hybrid properties of g-CNTC structure; graphene foliates from the CNT out-sidewalls provides a way to optimize the hybrid structure, allowing for higher charge

generates for superior electronic conductivity and electrocatalytic properties than any of the two materials could achieve on their own. In this work, we will synthesis g-CNTC via single-step process of FCCVD method. Subsequently, the produced hybrid will be incorporated with the binders to form a slurry paste and eventually deposited for CE film. Therefore, this work study the effect of g-CNTC microstructure on electrical and electrocatalytic properties to improve the power conversion efficiency. Then the performance in terms of power conversion efficiency was compared with standard CNTP and Pt catalysts.

Materials and Methods

The materials used to synthesis g-CNTC and CNTP were supplied from the following providers: ferrocene (98%) Sigma Aldrich, thiophene (99%) Alfa Aesar, and ethanol Hmbg. Meanwhile, materials for DSSC fabrication were ethylcellulose (48% ethoxyl), hexachloroplatinic acid hexahydrate purchased from Sigma Aldrich. Alpha-terpineol (97%) was obtained from Acros Organics. The Fluorine doped tin oxide (FTO) coated glass with a sheet resistance <15 Ω/sq was supplied from Zhuhai Kaivo Optoelectronic Technology Co., Ltd. The soda-lime glass was supplied from Sigma Aldrich. Ti-Nanoxide (TiO_2) D/SP paste, ruthenium complex (N719) dye, and surlyn polymer was supplied from Solaronix Switzerland.

The synthesis of carbon nanotubes cotton via a floating-catalyst chemical vapor deposition technique. In this experiment, floating-catalyst chemical vapor deposition (FCCVD) technique used is simplified into a schematic diagram as Fig. 1. We introduced mixed gases of argon, Ar (200 sccm) and hydrogen, H_2 (100 sccm) as a carrier gas, thiophene as a growth rate enhancer, ferrocene as the catalyst, and ethanol as a carbon source. Ferrocene, and thiophene were firstly mixed in ethanol and sonicated for dispersion. The synthesis was started with argon flow at 200 sccm to eliminate the oxygen out from the furnace chamber at 600 °C until it reaches 1150 °C and, then changed to H_2 gas flow at 100 sccm during the reaction. The synthesis was then carried out using a syringe pump to inject carbon sources with a flow rate of 8 ml/h for 2 hours and other synthesis parameters such as temperature, catalyst precursor, and the gas flow rate were fixed. During the cooling process, H_2 gas was stopped and argon gas flow was used. A bulk of cotton was formed during the synthesis and then collected inside a collection chamber. A similar synthesis of our CNT was also reported in the literature [12], [15–17]. Eventually, a bulk of cotton was crushed using ball milling energy for 30 minutes to obtain powder g-CNTC and preparing it for conductive paste. The details of the conductive paste were prepared in the next section. The samples were then characterized using Field Emission Scanning Electron Microscopy (FESEM), Transmission electron microscope (TEM), four-point probe, and Raman spectroscopy respectively.

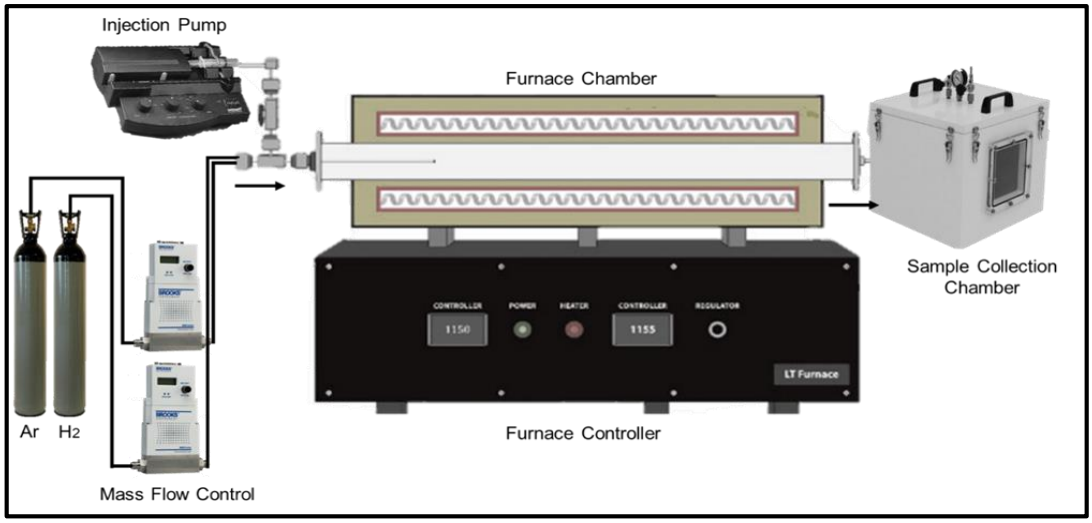

Figure 1. Schematic diagram of floating-catalyst CVD furnace.

Counter electrode preparation. The colloidal carbon was prepared using a simple mixing route. A weight ratio of 80 % binder to 20 % of carbon composition is prepared. Firstly, the mixture of carbon and the organic binder (ethylcellulose and α-terpineol) was vigorously stirred on the hot plate until the mixture become homogenous. The mixture was kept under stirring for 12 hours to ensure homogeneity and there was no agglomeration between the carbon and binder. Then, the paste was deposited onto a clean FTO glass using a Doctor Blade method. In this experiment, we used Scotch tape (3M, Scotch Magic Tape) by using different Scotch tape layers to control the thicknesses. The coated film was annealed in an air furnace at 500 °C for 30 minutes. A double layer of g-CNTC was deposited on the FTO substrate. Based on our initial measurement electrical properties reported in Table I, the layer is chosen based on the optimum electrical conductivity as double-layer g-CNTC obtained a good conductivity. Subsequently, the coated film was tested with its electrical conductivity, catalytic activity, and graphitization. In this work, the samples were labeled as g-CNTC and CNTP respectively. For comparison, the reference electrode was composed of the platinum deposited film and annealed at the same condition at 500 °C for 30 minutes.

DSCC device fabrication. The cleaned photoanode substrates were treated with ozone treatment for 10 min to remove impurities and activate the surface of the FTO layer. After that, the pre-treatment of the photoanode substrates were soaked in 40mM $TiCl_4$ solution under 80 °C for 1 hour. The process was carried out to improve the adhesion between TiO_2 and FTO glass as well as to reduce the recombination of the electrons. Then, the substrates were rinsed with DI water followed by annealing at 500 °C for 30 minutes. A photoanode was prepared by depositing the D/SP TiO_2 paste single layer on the FTO glass using a screen-printing method with a 0.25 cm^2 of TiO_2 active area. The deposited TiO_2 was dried for 20 minutes on the hotplate to prevent the active area from shocking thermal and cracking during the heat-treatment process. The coated film was annealed at 500 °C for 30 minutes. Subsequently, the photoanodes were treated again in 40mM TiCl4 using the same procedure. After the post-treatment of the photoanodes, they were immersed in 0.4mM of N719 dye for 48 hours at room temperature. Eventually, both photoanode and counter electrode were combined into the sandwich-like structure attached with the 60 µm surlyn spacer. The iodine electrolyte was injected into the solar cells device and immediately sealed both sides of the cell using UV-cured resin. These were to ensure the electrolyte evaporates into the air. The performance of the solar cells was tested under the solar simulator accordingly.

Results and Discussion

Morphological study of g-CNTC analysis. The morphology of the synthesized g-CNT and CNTP were carried out using FESEM (FEİ NovaNanoSem 230, Holland). The g-CNTC and CNTP synthesized via floating catalyst CVD at 1150 °C with 8 ml/hr of injection rate are displayed in Figure 2(a,b). The g-CNTC image shows a similar morphological structure as reported in previous work where it showed the g-CNTC formed longer, thread-like structure, and entangled with one another to form cotton structure [17,12]. The CNTP morphology showed a non-linear nanotubes growth due to insufficient sulfur during the synthesis. An average diameter of 40 nm indicating that the g-CNTC produced was multi-walled which consists of g-CNT perpendicularly oriented foliates growing out from the sidewalls of multiwall CNT [18,19].

Figures 2 (c) and (d) show the morphology of the g-CNTC and CNTP on FTO substrates. It can be observed that the particles are randomly distributed throughout the samples. The morphology of the g-CNTC electrode exhibits a large grain boundary that enables the redox reaction to diffuse effortlessly, and efficient electron transfer to increase the conductivity. The fundamental advantage of the hybrid g-CNT structure is the high surface area of three-dimensional framework of the CNTs coupled with the high edge density of graphene can significantly increase the total charge capacity per unit of nominal area as compared to other carbon nanostructures [20]. The TEM image in Figure 2(e) proved the additional insight of graphene foliates with both edges and basal planes of the CNT having an average foliates size of 137.88 nm. A bulk form of our synthesized g-CNTC is shown in Figure 2(f).

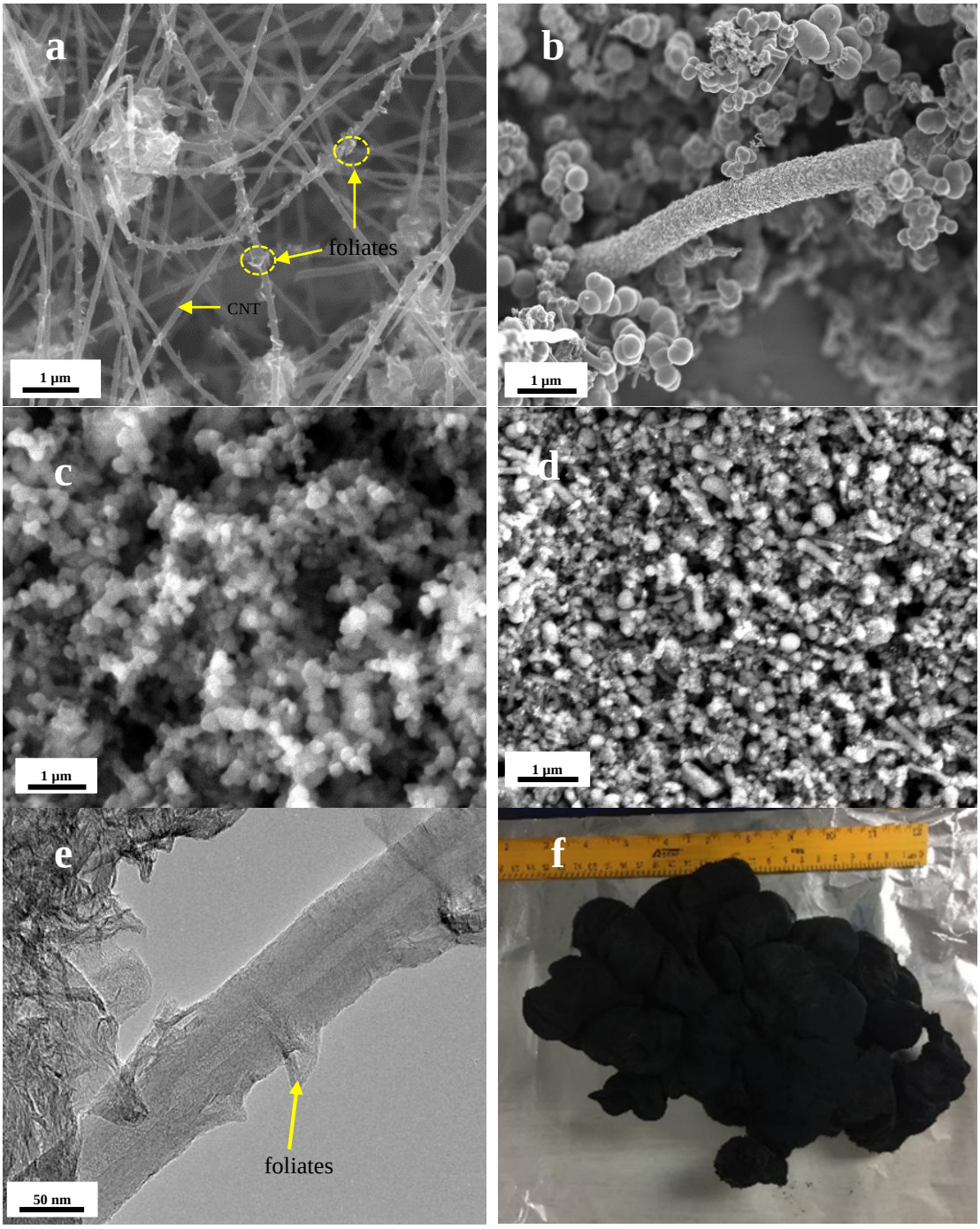

Figure 2. FESEM (a,b) g-CNTC and CNTP, (c,d) g-CNTC and CNTP on FTO substrates, (e) TEM images of g-CNTC and (f) optical micrograph as-synthesized g-CNTC

Raman spectra analysis. Raman spectroscopy (WITec, model Alpha 300R) with 488 nm of excitation wavelength was carried out to study the graphitization of the CNT. The Raman spectra as depicted in Fig. 3 revealed the G band's existence at around 1608 cm^{-1}, where the intensity is comparable to the D band at 1355 cm^{-1}. In Figure 3, peaks of the D band representing an sp^3 hybrid carbon a disordered feature of graphite structure, while the G band indicates sp^2 content in the sample. According to Dresselhaus [21], it is related to an sp^2 bond vibration of the carbon atoms in the 2D hexagonal lattice and, is coupled with a tangential stretching mode of graphite. The I_D/I_G ratio is used to determine the number of

structural imperfections that occured in the carbon materials. The lower I_D/I_G ratio approaching to zero represents a better quality of graphitization [22]. In this analysis, the g-CNTC and CNTP sample obtained a 0.98 and 0.89 intensity ratio, a slightly higher ratio obtained from lattice defects and the occurrence of other carbon materials such as uneven nanotubes occur in the samples.

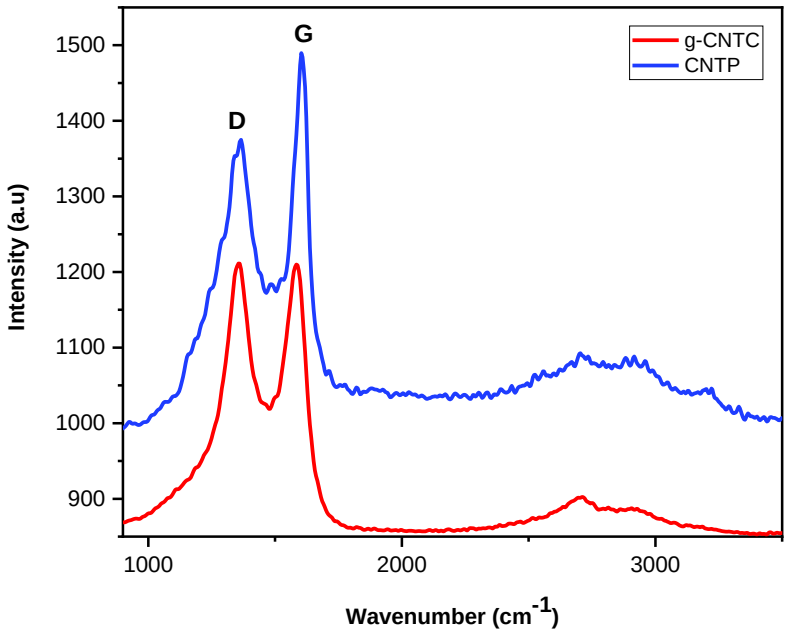

Figure 3. Raman spectra of CNTC and CNTP counter electrode.

Electrical conductivity analysis. The electrical conductivity of the counter electrode was determined using a four-point probe (Loresta-GX MCP-T700, Mitsubishi Chemical Analytech). The measurement was conducted using rectangular probes; 2 probes for voltage supplies and 2 probes for current. Table 1 shows a resistivity and conductivity of the g-CNTC and CNTP with thickness of 31 µm, 63 µm, 26 µm, and 58 µm respectively. The thicknesses of the films deposited on the FTO substrate were controlled using different numbers of Scotch tape layers from one to two layers and the thicknesses were measured using a 3D Laser Digital Microscope. The thickness of both samples increases as the resistivity decrease, a similar trend shows for both samples are related to graphitic properties [23]. The obtained resistivity and conductivity were confirmed by the equation: $R=\rho \frac{L}{Wt} = R_s \frac{L}{W}$, and $\sigma = \frac{1}{\rho}$; where R_s is the resistance when width (W) = length (L), t is the thickness, ρ is the resistivity and σ is the conductivity. The g-CNTC samples showed lower resistivity compared with CNTP resulted in higher conductivity, which showed that the electron movement is faster over the graphitic interfacial layers due to lower barrier resistance. Furthermore, due to the growth of graphene foliates at the sidewalls CNT, the chemical bond of these materials generates a more charge transfer resulting in excellent conductivity. The structural length difference between the g-CNTC and CNTP gives significance to the electrical properties, as the ability of a substance to transport electrical charge will be affected by its length variation. Based on these electrical properties, the only samples with higher thickness were proceeded in the fabrication of devices and electrochemical analysis due to good electrical conductivity**.**

Table 1. Comparison of thickness, resistivity and conductivity of g-CNTC and CNTP.

Samples	Layers	Thickness (μm)	Resistivity (Ω/cm)	Conductivity (Scm^{-1})
g-CNTC	Single	31	273	3.66×10^{-3}
	Double	62	155	6.45×10^{-3}
CNTP	Single	26	3.90×10^{3}	2.56×10^{-4}
	Double	58	780	1.28×10^{-3}

Electrocatalytic analysis. The catalytic activity of the carbon film was tested using cyclic voltammetry (CV) (Automatic Polarization System HSV-100, Hokuto Denko, Japan) to determine electrocatalytic behaviors of the counter electrode with the scan rate of 100 mV/s. In the CV analysis, a pair of redox peaks were obtained. The positive anodic side corresponds to the iodide oxidation, whereas the negative cathodic side belongs to triiodide reductions. The range of peak at 0.1-1.4 V showed iodide to triiodide reactions, and the peak at range of - 0.25 to -1.0 showed the reduction of triiodide to iodide. The electrochemical behavior of Pt, g-CNTC and CNTP counter electrodes is presented in Figure 4. The current density of g-CNTC electrodes at reduction peak is higher compared with CNTP and Pt electrodes, while CNTP and Pt electrodes having similar CV behavior. The higher current reduction peak of the g-CNTC electrode indicated that the electrode has a larger active surface to electrocatalyst occurs. In addition, the reduction peak of g-CNTC electrode is located to the positive side in the CV graph, suggesting that reduction reaction can occur at a lower overpotential, obtained a higher open-circuit voltage (V_{oc}) in DSSC performance accordingly. Therefore, the g-CNTC electrode is the most potential counter electrode due to excellent catalytic ability, meanwhile, the CNTP electrode is not suitable because of poor catalytic ability due to its poor electrical conductivity, attributed to the difficulties of electron mobility moving through larger barrier resistance [23].

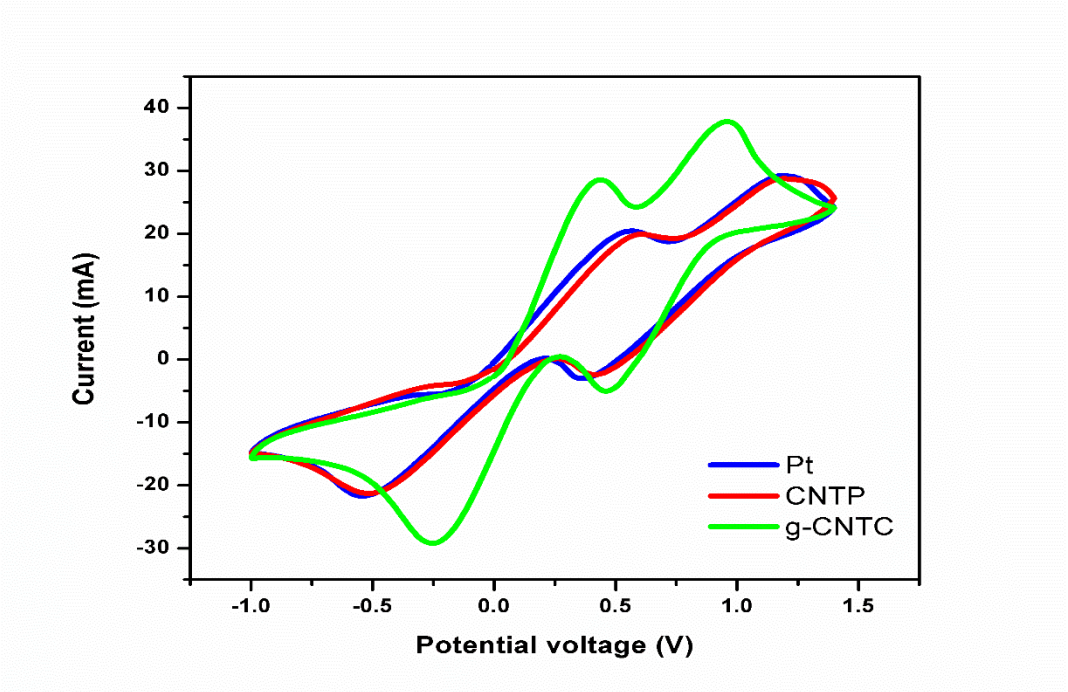

Figure 4. CV curves of g-CNTC, CNTP, and Pt counter electrodes

Photovoltaic measurement analysis. The DSSCs performance was conducted using a solar simulator (CEP-2000 Bunko Keiki Co. Ltd, Japan) equipped with the xenon lamp (Bunko Keiki BSO-X150LC) with an intensity of 100 mW/cm^2. The current-density voltage parameters of the carbon counter electrode and platinum DSSC are summarized in Table 2, while the current-density voltage curve of DSSC is presented in Figure 5. The g-CNTC sample shows the highest efficiency of 3.49%, while the standard CNTP and Pt with the efficiency of 2.93% and 3.12% respectively. Despite the high efficiency, the g-CNTC cells show comparable V_{oc} with platinum, CNTP shows a little bit higher V_{oc}. However, the short-circuit current density (J_{sc}) of CNTP is less than the DSSC with Pt and g-CNTC catalyst. The high J_{sc} owing to the contribution of the material directed to the increase of high catalytic ability of g-CNTC which cause quick redox reaction and photo-sensitized for efficient regeneration. This was supported by the CV analysis in Figure 4. The transparent Pt counter electrode obtained 11.51 mA/cm^2 of J_{sc}, consists of activated platinum on the FTO glass, reflected a portion of the unabsorbed incident solar light back to the TiO_2 photoanode, and generated more photocurrent. However, this result is entirely blocked in the opaque g-CNTC counter electrode and therefore has a low J_{sc} compared to the Pt counter electrode. The increase of V_{oc} of the g-CNTC and CNT is caused by the improvement of energy level conductive band in TiO_2 and the function of carbons to catalyze the excited electrons, thus enhancing the J-V of the whole device performance. The improvement in fill factor (FF) can be credited to the low resistance value at the counter electrode interface.

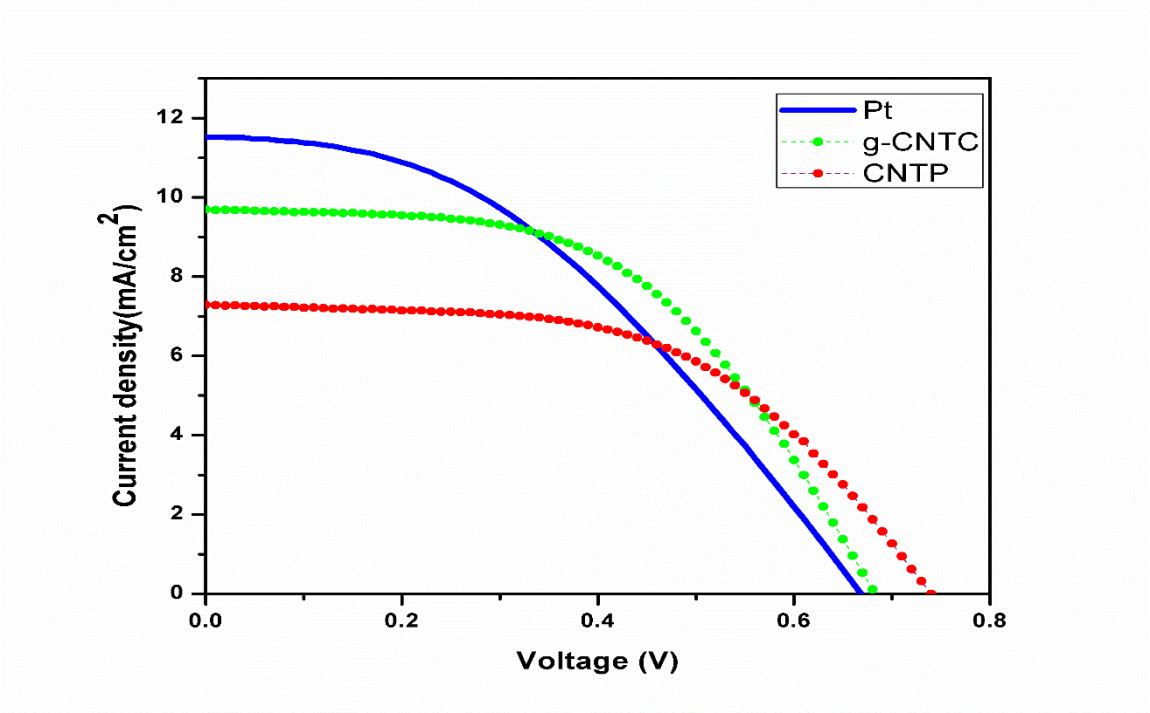

Figure 5. J-V curves of the various counter electrode of DSSC

Table 2. Current Density- Voltage (J-V) measurement.

Samples	J_{sc} (mA/cm^2)	V_{oc} (V)	FF	η (%)
g-CNTC	9.70	0.69	0.52	3.49
CNTP	7.29	0.75	0.54	2.93
Pt	11.51	0.67	0.40	3.12

Conclusion

In conclusion, this manuscript focuses on the potential of the electrocatalyst of g-CNTC for low-cost, good electrical conductivity, and electrocatalyst activity in DSSC applications. The morphology structure of the g-CNTC was longer with a diameter of 40 nm and straight nanotubes which can be correlated with the graphitic structure. Good conductivity was obtained as increase of thickness increased the conductivity due to the lower resistance barrier for electron mobility. Reduction of iodide/triiodide at the g-CNTC surface based on the electrochemical analysis, large surface-active area for the electrocatalyst occurred and this is responsible for the excellent electrocatalytic activity of g-CNTC electrode, and in turns improved the cell device performance to reach 3.49 % of efficiency. Hence, the g-CNTC can be a potential material to substitute conventional Platinum as the catalyst for DSSC.

Acknowledgments

The authors would like to thank the Institute of Nanoscience and Nanotechnology, Universiti Putra Malaysia for providing the experimental facilities. This study was funded by Universiti Putra Malaysia and Kyushu Institute of Technology Japan through (UPM-Kyutech/2019/9300465) grant.

Author Contributions

All authors contributed toward data analysis, drafting and critically revising the paper and agree to be accountable for all aspects of the work.

Disclosure of Conflict of Interest

The authors have no disclosure to declare.

Compliance with Ethical Standards

The work is compliant with ethical standards.

References

[1] Andualem, A. & Demiss, S. (2018). Review on Dye-Sensitized Solar Cells (DSSCs). *Edelweiss Appl. Sci. Technol.*, 2(1) 145-150.

[2] Ito, S., Murakami, T. N., Comte, P., Liska, P., Grätzel, C., Nazeeruddin, M. K. & Grätzel, M. (2008). Fabrication of Thin Film Dye Sensitized Solar Cells With Solar to Electric Power Conversion Efficiency Over 10 %. *Thin Solid Films*., 516(14) 4613-4619.

[3] Green, M. A., Dunlop, E. D., Levi, D. H., Hohl-Ebinger, J., Yoshita, M. & Ho-Baillie, A. W. Y. (2019). Solar Cell Efficiency Tables (version 50). *Prog. Photovoltaics Res. Appl*., 27(7) 565-575.

[4] Gong, J., Liang, J. & Sumathy, K. (2012). Review on Dye-Sensitized Solar Cells (DSSCs): Fundamental Concepts And Novel Materials. *Renew. Sustain. Energy Rev.*, 16(8) 5848-5860.

[5] Buda, S., Shafie, S., Abdul Rashid, S., Jaafar, H. & Khalifa, A. (2017). Response Surface Modeling of Photogenerated Charge Collection of Silver-Based Plasmonic Dye-Sensitized Solar Cell Using Central Composite Design Experiments. *Results Phys.,* 7 493-497.

[6] Sharif, N. F. M., Kadir, M. Z. A. A., Shafie, S., Rashid, S. A., Wan Hasan, W. Z. & Shaban, S. (2019). Charge Transport And Electron Recombination Suppression In Dye-Sensitized Solar Cells Using Graphene Quantum Dots. *Results Phys.*, 13 102171

[7] Lokman. M. Q., Shafie, S., Shaban, S., Ahmad F., Jaafar H., Mohd Rosnan R., Yahaya H. & Abdullah S. S. (2019). Enhancing Photocurrent Performance Based on Photoanode Thickness and Surface Plasmon Resonance Using Ag-TiO_2 Nanocomposites in Dye-Sensitized Solar Cells. *Materials Basel.,* 12(13) 2111.

[8] Hagfeldt, A., Boschloo, G., Sun, L., Kloo, L. & Pettersson, H. (2010). Dye-Sensitized Solar Cells. *Chem. Rev.,* 110(11) 6595-6663.

[9] Eisenberg, R. & Nocera, D. G. (2005). Overview of The Forum On Solar And Renewable Energy. *Inorg. Chem.,* 44(20) 6799-6809.

[10] Devadiga, D., Selvakumar, M., Shetty, P. & Santosh, M. S. (2021). Dye-Sensitized Solar Cell for Indoor Applications: A Mini-Review. *J. Electron. Mater.,* 50(6) 3187-3206.

[11] Yella, A., Lee, H.W., Tsao, H.N., Yi, C., Chandiran, A.K., Nazeeruddin, M.K., Diau, E.W.G., Yeh, C.Y., Zakeeruddin, S.M. & Grätzel, M. (2011). Porphyrin-Sensitized Solar Cells with Cobalt (II/III)-Based Redox Electrolyte Exceed 12 Percent Efficiency. *Science.,* 80(334) 629-633.

[12] Ismail, I., Mamat, S., Adnan, N. L., Yunusa, Z. & Hasan, I. H. (2019). Novel 3-Dimensional Cotton-Like Graphenated-Carbon Nanotubes Synthesized via Floating Catalyst Chemical Vapour Deposition Method for Potential Gas-Sensing Applications. *J. Nanomater.,* 2019 1-10.

[13] Wahyuono, R. A., Jia, G., Plentz, J., Dellith, A., Dellith, J., Herrmann-Westendorf, F., Seyring, M., Presselt, M., Andrä, G., Rettenmayr, M. & Dietzek, B. (2019). Self-Assembled Graphene/MWCNT Bilayers as Platinum-Free Counter Electrode in Dye-Sensitized Solar Cells. *ChemPhysChem*., 20(24) 3336-3345.

[14] Ratul, K. B., Nemala, S. S. & Mallick, S. (2019). Platinum and Transparent Conducting Oxide Free Graphene-CNT Composite Based Counter-Electrodes for Dye-Sensitized Solar Cells. *Surf. Eng. Appl. Electrochem.,* 55(4) 472-480.

[15] Ismail, I., Yusof, J. M., Mat Nong, M. A. & Adnan, N. L. (2018). Synthesis of Carbon Nanotube-Cotton Superfiber Materials. *Synthesis, Technology and Applications of Carbon Nanomaterials* (Elsevier Inc.) pp. 61-76

[16] Nur, I. I., Ismayadi, I., Shuhazly, M. M. & Adnan, N. L. (2019). Effect of Carbon Source Injection Rate on CNT Film via Floating Catalyst CVD Method. *Solid State Phenom.,* 290 113-121.

[17] Adnan, N. L., Ismail, I. & Hashim, M. (2015). Effect of Ferrocene Concentration on the Carbon Nanotube Cotton Synthesized Via Floating Catalyst CVD Method. *Aust. J. Basic Appl. Sci.,* 9(12) 109-113.

[18] Li, W. Z., Wen, J. G., Sennett, M. & Ren, Z. F. (2003). Clean Double-Walled Carbon Nanotubes Synthesized By CVD. *Chem. Phys. Lett.,* 368(3-4) 299-306.

[19] Abdallah, B., Elhissi, A. M. A., Ahmed, W. & Najlah, M. (2020). Carbon Nanotubes Drug Delivery System For Cancer Treatment. *Advances in Medical and Surgical Engineering* (Elsevier Inc.) pp. 313-332.

[20] Parker, C. B., Raut, A. S., Brown, B., Stoner, B. R., & Glass, J. T. (2012). Three-Dimensional Arrays of Graphenated Carbon Nanotubes. *J. Mater. Res.,* 27(7) 1046-1053.

[21] Dresselhaus, M. S., Jorio, A., Hofmann, M., Dresselhaus, G. & Saito, R. (2010). Perspectives on Carbon Nanotubes And Graphene Raman Spectroscopy. *Nano Lett.,* 10(3) 751-758.

[22] Wepasnick, K. A., Smith, B. A., Bitter, J. L. & Howard D. F. (2010). Chemical And Structural Characterization Of Carbon Nanotube Surfaces. *Anal. Bioanal. Chem.,* 396(3) 1003-1014.

[23] Collins, P. G., Zettl, A., Bando, H., Thess, A. & Smalley, R. E. (1997). Nanotube Nanodevice. *Science*, 278(5335) 100-103.